

---

**PHARMACEUTICAL TECHNOLOGY**

---

**THE INFLUENCE OF LOW PROCESS TEMPERATURE  
ON THE HYDRODYNAMIC RADIUS OF POLYNIPAM-CO-PEG  
THERMOSENSITIVE NANOPARTICLES PRESUMED AS DRUG CARRIERS  
FOR BIOACTIVE PROTEINS**WITOLD MUSIAŁ<sup>1\*</sup> and JIŘÍ MICHÁLEK<sup>2</sup><sup>1</sup>Department of Physical Chemistry, Wrocław Medical University, Borowska 211, 50-556 Wrocław, Poland<sup>2</sup>Department of Polymer Gels, Institute of Macromolecular Chemistry of the Academy of Sciences of Czech Republic, Heyrovského nám. 2, 162 06 Praha 6 – Břevnov, Czech Republic

**Abstract:** The aim of the work was to evaluate the influence of low process temperature on the hydrodynamic radius of the synthesized nanoparticles presumed for incorporation of bioactive proteins. The reaction prompted in temperatures of 22, 38 and 70°C. The first one reflected the ambient environmental temperature, at which the bioactive proteins may be implemented into the reactant mixture. The intermediate temperature should enable safe use of proteins during the reaction, and represents the upper limit of applied heat, due to the consequent denaturation of proteins at elevated temperatures. The reactant mixture heated up to 70°C provides excellent formation of nanoparticles, however the albuminous components will tend to degrade. Within the study we applied N,N,N',N'-tetramethylethane-1,2-diamine as an accelerator in the presence of the strong oxidizing agent – ammonium persulfate as radical initiator. Six batches of N-isopropylacrylamide derivatives with polyoxyethylene glycol diacrylamide co-monomer of molecular weight in the range of 2000 Da were synthesized within the course of surfactant free precipitation polymerization. The nanodispersions were assessed in the terms of hydrodynamic radius, by the dynamic light scattering method (DLS). The polydispersity index, as well as average hydrodynamic radius, and hydrodynamic radius of main population of particles, identified in the DLS device, were evaluated and discussed in the perspective of application of the nanogels as drug carriers for bioactive proteins.

**Keywords:** nanogel, N-isopropylacrylamide, thermosensitivity, protein stability, PEG

Controlled and targeted drug delivery in the case of proteins is developed intensively, due to the instable properties of the polypeptides in elevated temperatures. The model polypeptides e.g., insulin, BSA,  $\beta$ -galactosidase, calcitonin, lysozyme, and interleukin are loaded to the thermoresponsive nanogels, however the loading process is often ineffective (1, 2). Another approach includes the polymerization *in situ* with biologically active component implemented into reacting mixture (3). One of the attractive monomers applied in the studies on new polymeric drug carriers is N-isopropylacrylamide (NIPA) (4). Nanogels synthesized using NIPA enjoy a growing interest among specialists in drug form technology, bioengineering and biocompatible polymers. This is due to the fact of removal large amounts of water from particles of poly-N-iso-

propylacrylamide (polyNIPA), around volume phase transition temperature (VPTT). Consequently, one can expect the release of drug substance from the nanogels of polyNIPA under the influence of the thermal factor. Importantly, the VPTT is in the range of known physiological temperatures, e.g., in the range of the temperature of human skin surface. By modifying the composition and structure of derivatives of NIPA it is possible to obtain a number of macromolecules with programmed VPTT in the water system (5–7). The homogenous nucleation NIPA with co-monomers is usually performed at increased temperature (8), due to the fact that the key requirement for formation of the polymer in the microgel structure, is the insolubility of the obtained entity in the solvent, otherwise the macrogel will be obtained (9). The process uses an initiator, e.g.,

---

\* Corresponding author: e-mail: witold.musial@gmail.com

ammonium persulfate (APS), yielding initiator radicals imparting surface-active properties to the particles of the growing polymer chain. Macromolecules prepared by this technique are stabilized by covalently bound sulfate groups of the radical species derived from the persulfate ion (10). The obtained nanostructures collapse *in situ* in the process conditions, so the definite nanogel structures are obtained. However, in this procedure, the temperature increases beyond the VPTT of the obtained material, so the incorporation of thermally instable protein entities is hardly possible in the course of the polymer synthesis. Rarely, the proteins of interesting prospective applications are thermally stable at temperatures beyond the physiological human body temperature. Moreover, few of them are stable in the temperature range of 60–80°C, which is suitable for the process of synthesis of nano- and microgels in aqueous conditions. For example, glyceraldehyde-3-phosphate dehydrogenase produced by *Bacillus stearothermophilus* is stable in the range of 40–65°C, however the human one is degraded by 37°C (11). Due to that fact, some studies were developed to enhance the stability of bioactive proteins at elevated temperatures, however the practical application of modified thermally stable proteins in drug delivery, seems to be a very future task – some of the approaches include modification of the internal composition of the protein, or attachment of the proteins to the protective components (12–16). Another way of overcoming the problem of implementation of bioactive proteins into the polymer bead, in the polymerization course, is use of low process temperatures.

During the growth of the polyNIPA, several structures may be formed due to various bibliographic reports and process conditions. Saunders proposed some possible structures: homogenous,

core-shell with uniform mesh size in the core and the shell, agglomerated, and agglomerated with core-shell microgels (17). The additional important factor, which influences the formation of nano- and microstructures is micellization (18). When the room temperature is applied in the polymerization course, the growing polyNIPA chains do not shrink, and additionally, the number of active polymerization loci may be decreased, comparing to the increased process temperature. The low temperature and low initiator content result in structures of high radius and low density. This may lead to the growth of macrogels, instead of microgel or nanogel. Anyway, the problem of synthesis of nanogels and microgels, in the conditions providing the thermal stability of proteins, is very attracting to the researchers. An attempt was made to resolve the problem applying the initiator system consisting of APS with N,N,N',N'-tetramethylethane-1,2-diamine (TEMED) for immobilization of avidin by one-pot copolymerization at temperature near VPTT (19). In several works authors evaluated the polyoxyethylene glycol diacrylates (PEGDA) and methacrylates as co-monomers with interesting properties (20).

The aim of the work was to evaluate the influence of thermal conditions on the hydrodynamic radius of polyNIPA-co-PEGDA nanogels synthesized at various temperatures in the presence of APS-TEMED initiator system.

## EXPERIMENTAL

### Materials

N-isopropylacrylamide (NIPA), polyethylene glycol diacrylate of molecular mass ca. 2000 (PEGDA), N,N,N',N'-tetramethylethane-1,2-diamine were purchased from Aldrich (Prague, Czech

Table 1. The feed composition of the substrates in surfactant free precipitation polymerization; NIPA – N-isopropylacrylamide, PEGDA – polyoxyethylene glycol diacrylate of molecular weight ca. 2000 Da, TEMED – N,N,N',N'-tetramethylethane-1,2-diamine, APS – ammonium persulfate.

Nanogel type	Acronym	Substrates [g]			
		NIPA	PEGDA	TEMED	APS
polyNIPA-co-PEGDA (1 : 22)	PA	0.720	0.250	0.010	0.020
polyNIPA-co-PEGDA (1 : 38)	PB	0.720	0.250	0.010	0.020
polyNIPA-co-PEGDA (1 : 70)	PC	0.720	0.250	0.010	0.020
polyNIPA-co-PEGDA (2 : 22)	PD	0.720	0.250	0.020	0.040
polyNIPA-co-PEGDA (2 : 38)	PE	0.720	0.250	0.020	0.040
polyNIPA-co-PEGDA (2 : 70)	PF	0.720	0.250	0.020	0.040

Republic). APS was supplied by Lachema (Prague, Czech Republic). The substrates obtained from commercial suppliers were used without further purification. A dialysis bag with a molecular weight cut-off of 12000–14000 Da was received from Sigma Aldrich (Prague, Czech Republic). Deionized water was produced in TKA DI 6000 system (Niederelbert, Germany) and we used it in all following procedures.

### Synthesis of the thermosensitive nanoparticles

The surfactant-free precipitation polymerization (SFPP) was performed to obtain polyNIPA nanogel particles crosslinked by PEGDA. The polymerization was performed in deionized water under an inert nitrogen atmosphere according to the procedure evaluated by Pelton and Chibante (21, 22), and developed in groups of Snowden and Vincent (23–25). The radical initiator, APS, was placed in a 500 mL, three-necked round-bottomed flask and stirred continuously at 120 rpm. Pre-dissolved NIPA and cross-linking agent PEGDA were dissolved in 20 mL of deionized water with stirring and were then added to the reaction vessel. After 4 h, the dispersion was cooled to room temperature and filtered. Dry weight analysis of the nanogels showed the dispersion to have a concentration on the order of 0.1–0.5 wt.%. The starting composition of the substrates is given in Table 1, with respective acronyms of the nanodispersions.

### Equilibrium dialysis – purification of nanogels

Dialysis – purification by diffusion through semipermeable membrane was performed in the set of glass vessels. The sample of 50 mL of nanogel dispersion was closed in dialysis bag, and transferred into 300 mL glass vessel. The system was stirred in IKA-VIBRAX-VXR device (Germany), at 100 rpm. The particles were dialyzed against deionized water until the conductivity was less than 1.0  $\mu\text{S}/\text{cm}$  (26). Within the first 30 h the conductivity in the acceptor compartment was measured and the water remained unchanged in the acceptor compartment. After 30 h, the water was replaced in acceptor compartment by fresh deionized water, and the conductivity measurement was taken after 24 h. The procedure was repeated every 24 h, through 18 days, till the conductivity did not exceed 1.0  $\mu\text{S}/\text{cm}$ .

### FTIR evaluations

Fourier transformed infrared spectra – FTIR of the obtained polymers were measured at ambient temperature with a Nicolet Nexus 870 FTIR spectrometer purged with dry air, and equipped with a

Golden Gate device ATR, with reproducible approximate sample loads of 3 kbar. Samples were measured in the dry state; the spectra were corrected for absorption of the solvent and  $\text{H}_2\text{O}$  vapors.

### Assessment of the hydrodynamic radius

The hydrodynamic radius was assessed in aqueous dispersions by dynamic light scattering (DLS). From the ca. 50 mL sample, 50  $\mu\text{L}$  was taken, and centrifugated within the Eppendorf tube filled with 1.0 mL of prefiltered water, in Roth MicroCentrifuge, at 6000 rpm for 45 min. From the tube 50  $\mu\text{L}$  of supernatant were taken, and placed into polystyrene-single use fluorimeter cuvettes. Then, 1 mL of de-ionized water, filtered through 0.2  $\mu\text{m}$  PVDF Whatmann nanofilter, was added to the cuvette and the sample was inserted into Zeta Sizer Nano with 173° backscatter measurement arrangement and settings of Mark-Houwkin parameters. The duration of measurements was extended for the case of large particles, with relaxation time multiplier of 100000. The measurements settings were automated to seek optimum position; the attenuator selection was also automated. Every measurement was multiplied five times. Three sets of data were excavated from every measurement: (1) average radius of the nanogels counted on the total measured nanogels ( $R_{\text{ha}}$ ), (2) radius of the main fraction of nanogels present in the evaluated spectrum of sizes in the assessed dispersion ( $R_{\text{hm}}$ ), and (3) polydispersity index of the assessed dispersions of thermosensitive nanogels (PI) in the Zetasizer Nano Software Version 5.03.

## RESULTS

Due to the FTIR assessments within all the products, the polyNIPA polymer was synthesized in all the cases with implemented PEGDA crosslinker, as confirmed in previous work (12). The yield of the reaction was different, and depended on the applied conditions and feed compositions. The yields of nanogels PA-PF, estimated due to the gravimetric assessments, were in the range of 8–93%. The proposed structure of the obtained nanogel is visualized in Figure 1.

The measurements of synthesized nanogels performed *via* DLS give characteristic set of data, which is valuable in the terms of evaluation of the structure of thermosensitive macromolecules obtained on the basis of NIPA. We assessed in details three parameters in pure aqueous environment, as it is mentioned above: (1) average radius of the nanogels counted on the total measured nanogels

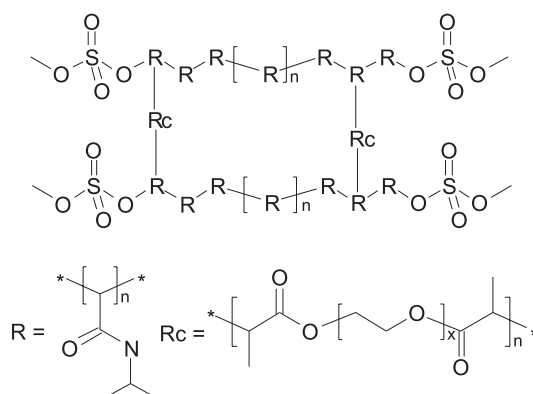


Figure 1. Visualization of proposed structure of the synthesized nanogels PA-PF

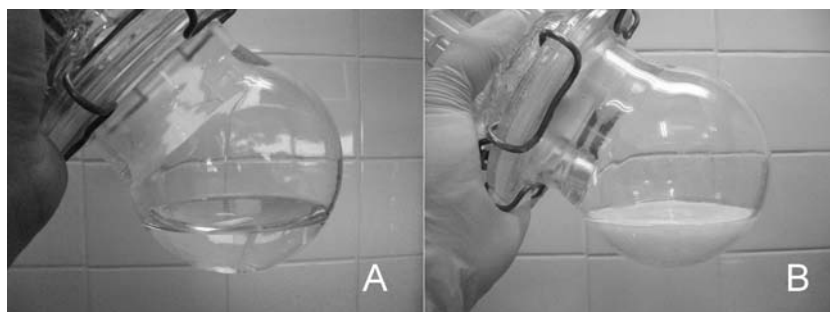


Figure 2. The synthesized system PD below (A) and over (B) VPTT

( $R_{ha}$ ), (2) radius of the main fraction of nanogels present in the evaluated spectrum of sizes in the assessed dispersion ( $R_{hm}$ ), (3) polydispersity index of the assessed dispersions of thermosensitive nanogels (PI). In the macroscopic view, the dispersions may be defined as transparent below the VPTT, whereas at increased temperatures they are non-transparent, due to the aggregation of small particles as it is presented in Figure 2 for the system pilot PD synthesized in our laboratory.

The general observation of the data leads to the conclusion, that the radii at fixed temperature are higher in the case of lower concentration of the initiator/accelerator system, with the exception of the systems PA and PD. In the case of the both latter nanogels (PA, PD) the effective size, measured in DLS conditions, is better presented when the extreme values are rejected from the considerations.

#### Hydrodynamic radius of microspheres prepared at 22°C

The  $R_{ha}$  of nanogels synthesized in the temperature of 22°C, was in the range between 98 and 245

nm, and it was not possible to distinguish between the batch PA and PD in the entire range of evaluated temperatures of measurements i.e., 10–52°C. Notwithstanding, we noted the characteristic shape of the polynomial trend line, which took the form of obverse letter U. The average radii are presented in Figure 3A. When the extreme values were rejected from the considerations, we observed a decrease of radius, which is typical for the thermosensitive N-isopropylacrylamide derivatives as it is visualized in Figure 3B ( $R_{hm}$ ). Notwithstanding, the diversity of radii was high.

#### Hydrodynamic radius of microspheres prepared at 38°C

The concentration of initiator influenced the direction of the  $R_{ha}$  changes, in the batches prepared in intermediate temperature of the synthesis (PB, PE). In PB batch, the  $R_{ha}$  increased slightly with increased temperature from ca. 183 nm at 10°C to 228 nm at 52°C, while the PE presented opposite tendency – the  $R_{ha}$  decreased with the increase of the temperature in the course of the size assessments

from 432 nm to 40 nm – Figure 4A. Similarly, the values of hydrodynamic radius after rejection of extreme values –  $R_{hm}$ , also decreased in the range between 1360 nm and 50 nm for PE. The batch PB did not change significantly the radius with the alteration of the temperature – the initial and final value corresponded, respectively, to 176 nm and 128 nm, as it is presented in Figure 4B.

#### Hydrodynamic radius of microspheres prepared at 70°C

The values from  $R_{ha}$  measurements performed on nanogels prepared at temperature of 70°C are gathered in Figures 5A and 5B. The PC batch has higher radii both in the case of initial and final temperature, i.e., 98 nm and 50 nm, comparing to the batch PF, with initial and final values of  $R_{ha}$  89 and 47 nm, respectively (Fig. 5A). The initial values of  $R_{hm}$  were in the range of 110 nm for PC and 105 nm for PF, while the final values were 55 nm and 52 nm, respectively (Fig. 5B).

#### Polydispersity index

The PDI factor is illustrated on the Fig. 6A–6C. For the nanogels synthesized in temperature of 22°C the PDI is below the VPTT in the range of 0.01–0.37. The highest values were observed in the case of nanogels obtained in SFPP prompted in temperature of 38°C. Interestingly, the highest values of 1.0 were observed below VPTT for the the batch PE with high content of TEMED and APS, while over VPTT the highest values were observed in the case of PB with lower content of TEMED and APS. The nanogels obtained in the temperature of 70°C were characterized by highest homogeneity and the PDI did not exceed the range of 0.09–0.167 in the case of PF, and 0.04–0.164 in the case of PC, with exception of one point for PC equal to 0.249.

#### DISCUSSION

The often misleading notion “size” usually is referred in nanoscience to the hydrodynamic diame-

Table 2. Evaluation of the average hydrodynamic radii obtained in the DLS measurements.

Shift of average hydrodynamic radius ( $R_{ha}$ ) with increase of temperature			
Concentration of initiator [mg/L]	Temperature of synthesis	Acronym	Change of radius of the nanogels, when the VPTT is crossed
TEMED: 10 APS: 20 (○)	22	PA	Similar radii, high diversity of radius, $\cap$ shape
	38	PB	Slight increase
	70	PC	Typical decrease
TEMED: 20 APS: 40 (●)	22	PD	Similar radii, high diversity of radius, $\cap$ shape
	38	PE	Decrease, L shape
	70	PF	Typical decrease

TEMED: N,N,N,N-tetramethylethane-1,2-diamine, APS: ammonium persulfate, PA-PF: synthesized nanoparticles, the descriptors (○), and (●) represent respective values on the Figures throughout the entire text.

Table 3. Evaluation of the hydrodynamic radii of main fraction of nanogels obtained in the DLS measurements.

Shift of hydrodynamic radius of main fraction of nanogels ( $R_{hm}$ ) with an increase of temperature			
Concentration of initiator [mg/L]	Temperature of synthesis	Acronym	Change of radius of the nanogels, when the VPTT is crossed
TEMED: 10 APS: 20 (○)	22	PA	Decrease of radius, high diversity of radius
	38	PB	Similar radii, not shifted
	70	PC	Typical decrease
TEMED: 20 APS: 40 (●)	22	PD	Decrease of radius, high diversity of radius
	38	PE	High decrease
	70	PF	Typical decrease

TEMED: N,N,N,N-tetramethylethane-1,2-diamine, APS: ammonium persulfate, PA-PF: synthesized nanoparticles, the descriptors (○), and (●) represent respective values on the Figures throughout the entire text.

ter, or hydrodynamic radius. Due to the works of Dušek, the number of macromolecules obtained *via* SFPP, may increase with the parallel increase of initiator concentration (27–29). If the reacting systems consist of the same amount of monomer, but the concentration of the initiator increases, parallel the hydrodynamic radius of obtained macromolecule should decrease. The DLS system gives an opportunity to measure the hydrodynamic radius. Respectively, the DLS measurements should enable evaluation of the influence of the initiator concentration on the “size” of obtained nanogels. In Tables 2 and 3 we present the evaluated data in compact form.

The evaluation of  $R_{ha}$  gives an assumption, that the nanogels prepared at the 22°C are very varied in the terms of hydrodynamic radius. However, when the extreme data are excluded, the main fraction of the nanogels may be assigned to the range 138–235 nm at the temperature below VPTT, and respectively, to the range 53–153 nm at temperature overcoming VPTT. This result confirms the possibility of synthesis of thermosensitive co-polymer of NIPA and PEG in temperature below the values critical for the denaturation of the proteins. The PDI measured throughout the entire assessment process increased

(Fig. 6A), due to the fact of aggregation of the particles in the region of VPTT (Fig. 3A), according to the decrease of the size of the main fraction of the nanogels in the course of the heating (Fig. 3B).

The complications arise when the SFPP process is performed at the temperature of 38°C. This temperature would be acceptable for implementation of some proteins into the SFPP process, however the resulting nanogels are highly differentiated, due to the high PDI. In the polymeric system PB with low content of accelerator and initiator the nanogels aggregated when the temperature increase (Fig. 4A), and we did not observe any precise VPTT, however due to the measurements of  $R_{hm}$ , the main fraction of the macromolecules was practically thermally insensitive (Fig. 4B). At the temperature below VPTT in the polymeric system PE dominate the huge structures with radius in the range of 746–1360 nm, but in higher temperature they disaggregate to more homogenous macromolecules in the range of 50–100 nm, with PDI decreased to values not exceeding 0.437 – Fig. 5B. The uncertain results of the synthesis at the temperature of 38°C confirm the multilateral form of the NIPA in the region of VPTT – the nascent polymer may be formed in various shapes according to Wu and Wang (27), and var-

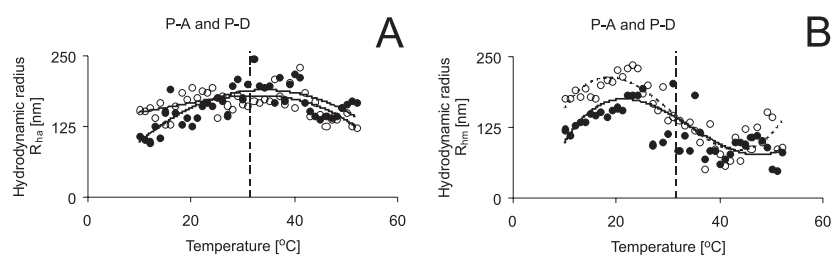


Figure 3. The influence of temperature on the average hydrodynamic radius ( $R_{ha}$ , **A**), and on the hydrodynamic radius of main fraction ( $R_{hm}$ , **B**) of nanogels obtained in the SFPP process, performed in the temperature of 22°C, respectively, at low (○) and high (●) concentrations of the accelerator/initiator system, the vertical discontinuous straight line represents VPTT, the dotted lines are the guides for the eye

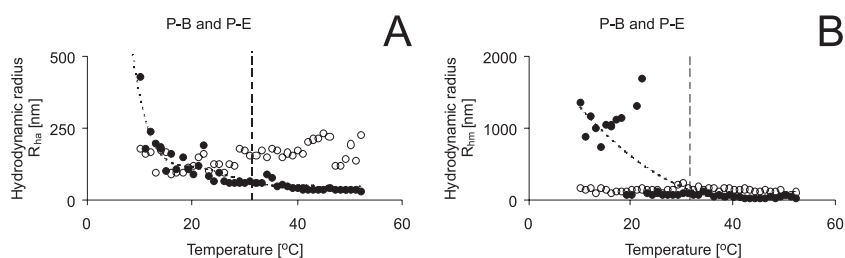


Figure 4. The influence of temperature on the average hydrodynamic radius ( $R_{ha}$ , **A**), and on the hydrodynamic radius of main fraction ( $R_{hm}$ , **B**) of nanogels obtained in the SFPP process, performed in the temperature of 38°C, respectively, at low (○) and high (●) concentrations of the accelerator/initiator system, the vertical discontinuous straight line represents VPTT, the dotted lines are the guides for the eye

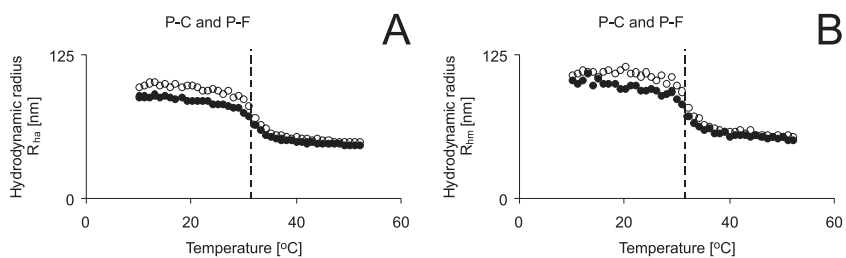


Figure 5. The influence of temperature on the average hydrodynamic radius ( $R_{ha}$ , **A**), and on the hydrodynamic radius of main fraction ( $R_{hm}$ , **B**) of nanogels obtained in the SFPP process, performed in the temperature of 70°C, respectively, at low (○) and high (●) concentrations of the accelerator/initiator system, the vertical dotted line represents VPTT

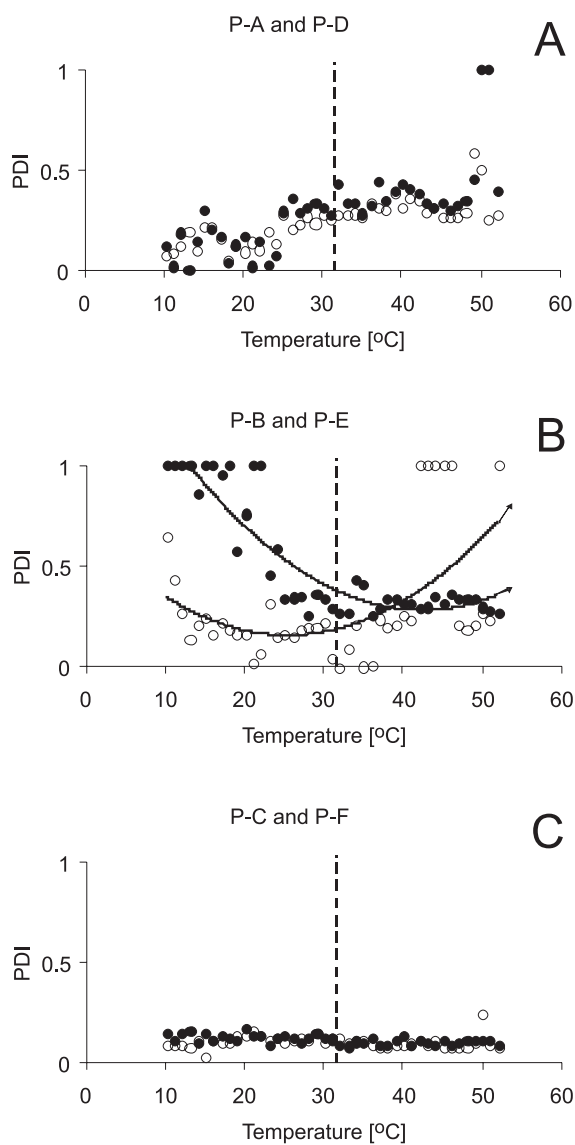


Figure 6. Polydispersity index of nanogels PA-P6, the vertical discontinuous straight line represents VPTT, the dotted lines are the guides for the eye

ious fractions of polymer may exist in this intermediate temperature, leading to high polydispersion.

Due to Wu and Wang (30), there are at least four thermodynamically stable states of a homopolymer chain in the coil-to-globule and the globule-to-coil transitions. At the low temperatures the particle is in the, so called, coiled state, and the chains movement is not hindered by molecular hindrances, what was confirmed in the work of Zhou et al. (31). On the opposite side, there is the, so called, globule state, when the chains of the macromolecule are definitively collapsed. However, between the two alternate states, two additional states are possible: crumpled coil, and molten globule. That phenomenon may explain the increase in  $R_{ha}$  value for the system PB and unsuspected high  $R_{hm}$  value for the PE system. The PB system was synthesized at intermediated temperature, when the growing polymer chain could be formed into crumpled coil or molten globule form. Moreover, the initiator system was in rather low concentration. Therefore, large particles were formed and the implemented crosslinker influenced growth of large and rigid structures, with tendency of aggregation. Also synthesis of PE system was prompted at interjacent temperature, however the increased initiator concentration should enhance the growth of large number of minor particles. From the graphs and the tables it is clear that at reduced temperatures the particles tend to aggregate, whereas after heating the particles are homogeneously dispersed in the medium. Their dimensions correlate with the assumption, that at increased initiator concentrations, the obtained nanoparticles should be smaller. The different behavior of PB and PE systems was confirmed also in terms of PDI – Fig. 6B. The system PB synthesized with low concentration of initiator tends to aggregate with the increase of temperature, so the PDI is increasing. In this case the long PEG chains may influence the increased interpenetration of the particles. The PE system tends to deaggregate at increased temperatures, due to the data from DLS.

The classical approach to the synthesis of the polyNIPAM-co-PEGDA system results in small particles – Fig. 5. They are in the radius range of ca. 100 nm – decreasing to ca. 50 nm after crossing the VPTT value. When the higher initiator concentration is applied, the particles seem to be slightly smaller, which is in agreement with the predictions of Dušek (24, 25) and Ciao (32). From the  $R_{ha}$  values, it may be deduced that in the batches of polyNIPAM-co-PEGDA : PC and PF rather small particles are present, as the respective values are slightly lower. The standard temperature applied for

the synthesis of polyNIPAM in the SFPP process is in the range of 70°C. The comparative graphs of size vs. environmental temperature confirm that the optimal conditions for synthesis of polyNIPAM-co-PEG are at elevated temperatures, however similar results were obtained in the case of PD, when the synthesis of the nanoparticles is performed at 22°C, however we recommend development of the TEMED/APS system for the further research in the SFPP at reduced temperatures, even much more below 38°C, and close to 22°C.

## CONCLUSIONS

The use of TEMED in the temperatures below the VPTT, and below the applied temperature of activation of the initiator, gives promising results at the temperature of 22°C. Due to our data, it is possible to synthesize thermosensitive nanogels, derivatives of NIPA and PEG in this low temperature conditions. When intermediate temperature 38°C is applied, with low concentration of TEMED and APS, the resulting nanogels tend to agglomerate, but they do not seem to be thermosensitive in the sense of typical polyNIPAM. The increased concentration of the accelerator and initiator favors synthesis of thermosensitive nanogels in the temperature of 38°C, but the produced nanogels are not homogeneous. The increased concentration of accelerator/initiator system promoted the decrease of the hydrodynamic radius in all the cases, irrespective of the temperature of measurement.

## Acknowledgments

The study was supported by research fellowship within “Development program of Wrocław Medical University”, Poland, funded from European Social Fund, Human Capital, National Cohesion Strategy, contract no. UDA-POKL.04.01.01-00-010/08-00 in 2011. The authors would like to thank to the following colleagues for the scientific and technical help in the performance of the measurements in the Institute of Macromolecular Chemistry in Prague, Czech Republic: František Rypáček, Petr Štěpánek, Karel Dušek, and Miroslava Dušková-Smrčková.

## REFERENCES

1. Bhuchar N., Sunasee R., Ishihara K., Thundat T., Narain R.: *Bioconjugate Chem.* 23, 75 (2012).
2. Bromberg L.E., Ron E.S.: *Adv. Drug Deliv. Rev.* 31, 197 (1998).

3. Ngwuluka N.: AAPS PharmSciTech 11, 1603 (2010).
4. Qiu Y., Park K.: Adv. Drug Deliv. Rev. 64, 49 (2012).
5. Quan C.Y., Wei H., Shi Y., Li Z.Y., Cheng S.X., Zhang X.Z., Zhuo R.X.: Colloid Polym. Sci. 289, 667 (2011).
6. Lee Y.J., Cheong I.W., Yeum J.H., Jeong Y.U.: Macromol. Res. 18, 208 (2010).
7. Dai W., Zhang Y., Du Z., Ru M., Lang M.: J. Mat. Sci. Mat. Med. 21, 1881 (2010).
8. Schild H.G.: Prog. Polym. Sci. 17, 163 (1992).
9. Pelton R., Hoare T.: in Microgel Suspensions, Fundamentals and Applications, 1<sup>st</sup> edn., Fernandez-Nieves A., Wyss H., Mattsson J. Eds., p. 11, Wiley-VCH, Weinheim 2011.
10. Odian G.: Surfactant Free Emulsion Polymerization: Principles of polymerization, p. 352, John Wiley and Sons, New Jersey 2004.
11. Vogt G., Woell S., Argos P.: J. Mol. Biol. 269, 631 (1997).
12. Menéndez-Arias L., Argos P.: J. Mol. Biol. 206, 397 (1989).
13. Kaushik J.K., Bhat R.: Protein Sci. 8, 222 (1999).
14. Wingreen N.S., Li H., Tang C.: Polymer 45, 699 (2004).
15. Noritomi H., Minamisawa K., Kamiya R., Kato S.: J. Biomed. Sci. Eng. 4, 94 (2011).
16. Prashar D., Cui D., Bandyopadhyay D., Luk Y.Y.: Langmuir 27, 13091 (2011).
17. Saunders B.R.: Langmuir 20, 3925 (2004).
18. Zheng S., Shi S., Xia Y., Wu Q., Su Z., Chen X.: J. Appl. Polym. Sci. 118, 671 (2010).
19. Hu X., Tong Z., Lyon A.: Langmuir 27, 4142 (2011).
20. Musial W., Kokol V., Fecko T., Voncina B.: Chem. Pap. 64, 791 (2010).
21. Pelton R.H., Chibante P.: Colloids Surf. 20, 247 (1986).
22. Pelton R.H.: Adv. Colloid Interface Sci. 85, 1, (2000).
23. Lowe J.S., Chowdhry B.Z., Parsonage J.R., Snowden M.J.: Polymer 39, 1207 (1998).
24. Nur H., Pinkrah V.T., Mitchell J.C.: Adv. Colloid Interface Sci. 158, 15 (2010).
25. Rasmusson M., Routh A., Vincent B.: Langmuir 20, 3536 (2004).
26. Senff H., Richtering W.: Colloid Polym. Sci. 278, 830 (2000).
27. Dušek K.: J. Polym. Sci. C, Polym. Symp. 16, 1289 (1967).
28. Dušek K.: J. Polym. Sci. C, 39, 83 (1972).
29. Dušek K.: Macromol. Chem. Macromol. Symp. 7, 37 (1987).
30. Wu C., Wang X.: Phys. Rev. Lett. 80, 4092 (1998).
31. Zhou S., Fan S., Auyeung S.C.F., Wu C.: Polymer 36, 1341 (1995).
32. Xiao X.C.: eXPRESS Polym. Lett. 1, 232 (2007).

*Received: 30. 10. 2013*